Thus there exists a direct correlation with contact angle data only for those cases where $\theta \simeq 0°$ and where the heat of immersion is of the order of ΔH_{sub}.[35] We can now see why the zero-order desorption onsets discussed above are unshifted. In both cases the minimum in the potential surfaces is that due to the water-water rather than the water-substrate interaction. It is not possible, in such instances, to probe these latter states directly with TPD.

Using these simple notions, it is apparent that the water-binding properties of the three polar surfaces (acid, amide, and alcohol) can be classified with regard to which potential dominates the TPD data; for the acid and amide it is clearly that due to the substrate-water interactions, while for the alcohol it is that due to the self-interaction of water. These latter insights also implicitly establish a structure-property correlation that would not be evident in a contact angle study (since $\theta \simeq 0°$ for each), namely the relative affinities of these surfaces for water: acid $\gtrsim$ amide $>$ alcohol. This suggests but one of the potential advantages which result from a consideration of data from both types of measurements. Even so, we advise caution in making extrapolations from one to the other. For example, it seems reasonable that there may exist surface reconstructions in these systems which might have an important bearing on interfacial properties in the temperature ranges appropriate to contact angle and solution phase reactivity studies; at the low temperatures used in TPD (necessary to operate in UHV) these same states might not be accessible. [8b,9]

(35) This does not take account of the complexities which might arise as a result of the temperature dependence of any of the relevant thermodynamic parameters, however.

Concluding Remarks

Our data suggest that certain conceptual analogies exist between contact angle behaviors (which measure macroscopic adsorption properties) and TPD profiles of microscopic UHV adsorption properties on these molecular surfaces. The desorption kinetics are complex in all instances and suggest that coverage dependences other than that related to simple mass action principles need to be considered. We present evidence that long-range dipolar interactions are important for at least water overlayers and that these interactions are, in fact, stabilizing.

Future papers will present additional examples of interfacial studies of such model organic solids as well as apply vibrational spectroscopy to the task of resolving several of the issues related to the complex molecular environments which exists at these interfaces and the structures formed by various overlayers.

Acknowledgment. We thank J. C. Tully for several illuminating discussions on the analysis of TPD data. We are also grateful to Professor G. Whitesides and his co-workers for their critical evaluation of an early draft of this manuscript. C. E. D. Chidsey and G. Scoles and his co-workers are also gratefully acknowledged for their communication of results prior to publication.

Through-Bond and Through-Space Interactions in a Series of Cyclic Polyenes

M. F. Falcetta,[†] K. D. Jordan,*[,†] J. E. McMurry,[‡] and Michael N. Paddon-Row*[,§]

Contribution from the Department of Chemistry, University of Pittsburgh, Pittsburgh, Pennsylvania 15260, Department of Chemistry, Cornell University, Ithaca, New York 14853, and School of Chemistry, University of New South Wales, P.O. Box 1, Kensington, New South Wales, 2033 Australia. *Received February 21, 1989*

Abstract: Electron transmission spectroscopy is used to determine the electron affinities of tetracyclo[8.2.2.2^{2,5}.2^{6,9}]-1,5,9-octadecatriene and pentacyclo[12.2.2.2^{2,5}.2^{6,9}.2^{10,13}]-1,5,9,13-tetracosatetraene. The electron transmission measurements indicate that the splittings between the π^* anion states of these compounds are at most a few tenths of an electronvolt. It is shown, with the assistance of ab initio molecular orbital calculations, that both through-bond (TB) and through-space (TS) interactions between the π^* (and π) orbitals of the above compounds and of tricyclo[4.2.2.2^{2,5}]-1,5-dodecadiene are sizable but that these two interactions oppose one another causing the net splittings in the π^* EA's and πIP's to be small. A simple perturbation molecular orbital model is presented which accounts for the trends in the IP's and EA's. Molecular orbital calculations are carried out which show that if the ethano bridges separating the ethylenic groups are replaced by trimethylene bridges, then the balance between the TB and TS effects is altered, and the splittings in the π^* and π manifolds are increased.

I. Introduction

The nature of the intramolecular interactions between functional groups in polyatomic molecules is a problem of fundamental importance. In the nomenclature of Hoffmann et al. such interactions may be classified as either through-space (TS) or through-bond (TB).[1] The former is a direct interaction and falls off rapidly with increasing separation between the groups. The latter involves a coupling through the connecting σ-bond framework and generally falls off slowly with the number of σ-bonds separating the functional groups.[1-3] In an orbital model, the net coupling between equivalent functional groups is associated with the splittings between the relevant molecular orbitals (MO's).

In the present study the interactions among the ethylenic π and π^* orbitals of tricyclo[4.2.2.2^{2,5}]-1,5-dodecadiene (**1**), tetracy-

[†] University of Pittsburgh.
[‡] Cornell University.
[§] University of New South Wales.

(1) Hoffmann, R.; Imamura, A.; Hehre, W. J. *J. Am. Chem. Soc.* **1968**, *90*, 1499. Hoffmann, R. *Acct. Chem. Res.* **1971**, *4*, 1. Gleiter, R. *Angew. Chem., Int. Ed. Engl.* **1974**, *13*, 696. Paddon-Row, M. N. *Acc. Chem. Res.* **1982**, *15*, 245.

(2) Balaji, V.; Ng, L.; Jordan, K. D.; Paddon-Row, M. N.; Patney, H. K. *J. Am. Chem. Soc.* **1987**, *109*, 6957. Paddon-Row, M. N.; Jordan, K. D. In *Molecular Structure and Energetics*; Liebman, J., Greenberg, A., Eds., 1988; Vol. 6, Chapter 3, p 115.

(3) Many researchers have concluded that through-bond interactions fall off exponentially with the number of bonds separating the chromophores. (See for example: Paddon-Row, M. N.; Cotsaris, E.; Patney, H. K. *Tetrahedron* **1981**, *42*, 1779.) Other functional forms for the dependence of these interactions with the number of bonds have been suggested. (For a recent review: Mikkelsen, K. V.; Ratner, M. A. *Chem. Rev.* **1987**, *87*, 113.) However, there is agreement on the key point that through-bond interactions generally fall off much more slowly with distance than do through-space interactions.

0002-7863/90/1512-579$02.50/0

clo[8.2.2.2^{2,5}.2^{6,9}]-1,5,9-octadecatriene (**2**), and pentacyclo-[12.2.2.2^{2,5}.2^{6,9}.2^{10,13}]-1,5,9,13-tetracosatetraene (**3**) are considered.

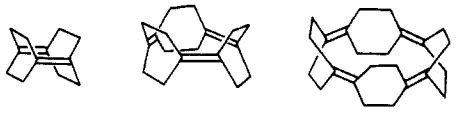

1 2 3

The ethylenic π and π^* orbitals of these compounds extend into the interior of the molecule, and as a result TS interactions should be sizable, particularly for **1** in which the two ethylenic groups face one another and are separated by only about 2.4 Å.[4] Since the ethylenic groups of **1–3** are separated by only three σ-bonds, TB interactions among the π and π^* orbitals are also expected to be important.

Photoelectron (PE) spectra have been determined for **1**,[4] **2**,[5] and **3**.[6] For **1** and **2** the PE spectra have been interpreted as indicating that the splittings in the π manifolds are quite small. Honneger et al. attributed the peak at 8.3–8.5 eV in the PE spectrum of the diene to ionization from both the $b_{1u}(\pi)$ and $a_g(\pi)$ orbitals.[4] This was confirmed by ab initio calculations carried out by these authors. The PE spectrum of the triene has peaks at 7.9, 8.1, and 8.3 eV. McMurry et al. attributed the 7.9-eV peak to ionization from the $a_1'(\pi)$ orbital and the 8.1- and 8.3-eV features to ionization from the $e'(\pi)$ orbitals, with the splitting between the latter arising from a Jahn–Teller distortion.[5] The assignments for **2** were supported by semiempirical MINDO/3 molecular orbital calculations. The PE spectrum of the tetraene has a broad feature centered near 7.9 eV which is apparently due to ionization from the $a_{1g}(\pi)$, $e_u(\pi)$, and $b_{1g}(\pi)$ orbitals.[6]

The present study employs electron transmission spectroscopy (ETS)[7,8] to determine the vertical electron affinities (EA) of **2** and **3**. To aid in the interpretation of the spectra, ab initio calculations are performed on the neutral molecules as well as on model systems consisting of ethylene molecules orientated as are the ethylenic groups in **1–3** but with the ethano (i.e., $-CH_2CH_2-$) bridging groups removed. The splittings in the π and π^* manifolds of the model systems are due primarily to TS interactions. In contrast, the orbital energies obtained from the calculations on **1–3** reflect both TS and TB interactions. Calculations are also carried out on analogues of **1** and **2** with the ethano bridges replaced by trimethylene bridges in order to change the relative importance of the TS and TB interactions.

II. Experimental Details and Results

In ETS one measures, as a function of electron energy, the derivative with respect to energy of the current of monoenergetic electron beam transmitted through the vapor of the species of interest. At those energies at which electron attachment occurs there is a rapid variation in the transmitted current and hence in the derivative. The vertical electron attachment energies are associated with the midpoints between the dips and peaks in the derivative spectra. The assumptions inherent in this procedure are discussed elsewhere.[9] The resolution of the spectrometer is about 0.05 eV, full-width at half-maximum (FWHM), and calibration of the energy scale is accomplished by reference to the onset of the beam as zero. For short-lived anion states, such as those studied here, the natural line widths may be several tenths of an electronvolt, making it difficult to resolve closely spaced anion states.

The ET spectra of the triene and tetraene, shown in Figure 1, each have a broad pronounced feature centered near 2.3 eV. The FWHM of this feature is about 0.8 eV in the triene and 1.2 eV

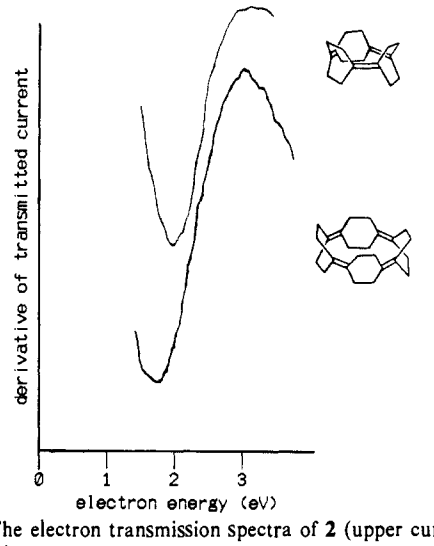

Figure 1. The electron transmission spectra of **2** (upper curve) and **3** (lower curve).

in the tetraene. For comparison we note that the π^* anion states of ethylene and 2,3-dimethylbut-2-ene have FWHM of about 0.8 eV.[10] These results suggest that the anion states of **2** are split by a relatively small amount ($\lesssim$0.1 eV) and that the anion states of **3** could be split by a few tenths of an electronvolt. The larger bandwidth of the 2.3 eV feature in the ET spectrum of **3** could also be caused by a larger Jahn–Teller coupling (in the ^2E_u anion state) in this case.

III. Ab Initio Calculations

All calculations were performed with the Hartree–Fock (HF) self-consistent field (SCF) procedure.[11] The geometries of the neutral molecule were fully optimized by using analytical gradients and the STO-3G basis set.[12] HF calculations using the 3-21G basis set[12] were also carried out on **1–3** at their HF/STO-3G optimized geometries. Assuming the validity of Koopmans' theorem (KT),[13] the IP's and EA's can be associated with the negatives of the energies of the filled and unfilled orbitals, respectively. This approach is clearly not suitable for obtaining absolute EA's.[14] However, previous work has shown that it is useful for predicting the trends in EA's[2,15] along a series of related compounds.

Of primary interest are the splittings between the various π (and π^*) orbitals of **1–3**. Table I summarizes the splittings obtained with both the STO-3G and 3-21G basis sets. For the filled π manifolds the two basis sets give the same orbital orderings and rather small net splittings. However, for the π^* manifold, the two basis sets give somewhat different results, with the STO-3G basis set giving relatively small splittings and the 3-21G basis set giving appreciably larger splittings in most cases. Since the 3-21G basis set is more radially extended than the STO-3G basis set, it should be more appropriate describing longer range interactions which could be more important in the anion states (or unfilled orbitals).[16] On the other hand, because the unfilled orbitals lie in the continuum for electron molecule scattering, there is the added problem of the virtual orbitals "collapsing" onto continuum

(4) Honneger, E.; Heilbronner, E.; Wiberg, K. B. *J. Electron Spectroc. Relat. Phenom.* **1983**, *31*, 369.
(5) McMurry, J. E.; Haley, G. J.; Matz, J. R.; Clardy, J. C.; Van Duyne, G.; Gleiter, R.; Schafer, W.; White, D. H. *J. Am. Chem. Soc.* **1986**, *108*, 2932.
(6) Gleiter, R. Unpublished Results.
(7) Sanche, L.; Schulz, G. J. *Phys. Rev. A* **1968**, *5*, 1972.
(8) Jordan, K. D.; Burrow, P. D. *Acc. Chem. Res.* **1978**, *11*, 341.
(9) Burrow, P. D.; Michejda, J. A.; Jordan, K. D. *J. Chem. Phys.* **1987**, *86*, 9.
(10) Jordan, K. D.; Burrow, P. D. *J. Am. Chem. Soc.* **1980**, *102*, 6882.
(11) The calculations were performed with the GAUSSIAN 86, Cray COS version, program of Binkley, J. S.; Frisch, M. J.; Raghavachari, K.; DeFrees, D. J.; Schlegel, H. B.; Whiteside, R.; Fluder, E.; Seeger, R.; Pople, J. A., Carnegie-Mellon University: Pittsburgh, PA.
(12) A discussion of and references to the STO-3G and 3-21G basis sets may be found in Hehre, W. J.; Radom, L.; Schleyer, P. v. R.; Pople, J. A. *Ab Initio Molecular Orbital Theory*; John Wiley & Sons: New York, 1986.
(13) Koopmans, T. *Physica (Amsterdam)* **1934**, *1*, 104.
(14) Not only does this approach neglect relaxation and correlation effects but also there is the additional problem that the anion states are embedded in the continuum for electron-molecule scattering. Calculations with flexible basis sets could end up describing continuum solutions rather than anion states. The use of a small basis set avoids this complication.
(15) Burrow, P. D.; Modelli, A.; Chiu, N. S.; Jordan, K. D. *J. Chem. Phys.* **1982**, *77*, 2699; see also ref 2.
(16) Burrow, P. D.; Jordan, K. D. *J. Am. Chem. Soc.* **1982**, *104*, 5247.

Table I. Through-Space (TS), Through-Bond (TB), and Net Orbital Splittings in **1**–**3**[a]

		splitting energies[b]						
		TS			TB		net	
compd		STO-3G	3-21G	6-31+G	STO-3G	3-21G	STO-3G	3-21G
diene	π^*	3.24	3.32		−3.23	−4.02	0.01	−0.70
	π	3.67	3.72	3.67	−3.35	−3.55	0.32	0.17
triene	π^*	2.35	2.13		−2.12	−1.39	0.23	0.74
	π	1.79	2.12	2.13	−1.97	−2.07	−0.18	−0.06
tetraene	π^*	1.06	1.30		−0.90	−0.31	0.15	0.99
		1.16	1.62		−1.02	−1.04	0.14	0.58
	π	0.71	0.93	0.93	−1.03	−1.15	−0.32	−0.22
		0.61	0.78	0.84	−0.87	−0.86	−0.26	−0.08

[a] The TS splittings are obtained from calculations on the model ethylene dimer, trimer, and tetramer systems. The TB interactions are obtained by subtracting these estimates of the TS splittings from the net splittings, obtained from the calculations on **1**, **2**, and **3**. [b] The splitting energies are taken to be positive for the case of pure TS interactions. [c] For the π^* orbitals the top row gives the splittings between the $a_{2g}(\pi^*)$ and $e_u(\pi^*)$ orbitals and the bottom row between the $e_u(\pi^*)$ and $b_{2g}(\pi^*)$ orbitals. For the π orbitals the top row gives splittings between the $b_{1g}(\pi)$ and $e_u(\pi)$ orbitals and the bottom row between the $a_{1g}(\pi)$ and $e_u(\pi)$ orbitals.

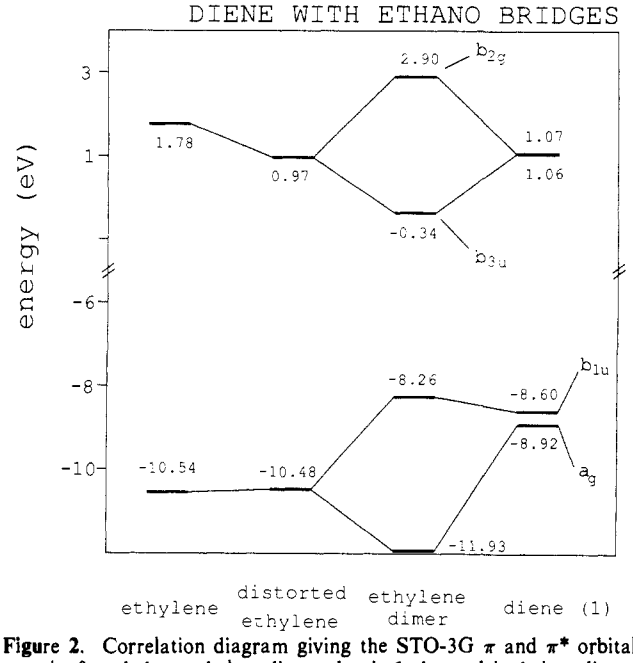

Figure 2. Correlation diagram giving the STO-3G π and π^* orbital energies for ethylene, ethylene distorted as in **1**, the model ethylene dimer, and the diene **1**.

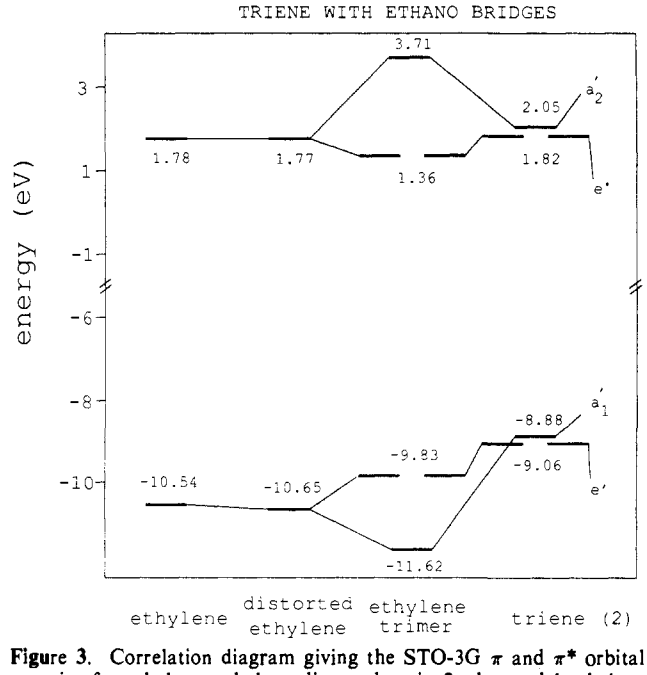

Figure 3. Correlation diagram giving the STO-3G π and π^* orbital energies for ethylene, ethylene distorted as in **2**, the model ethylene trimer, and the triene **2**.

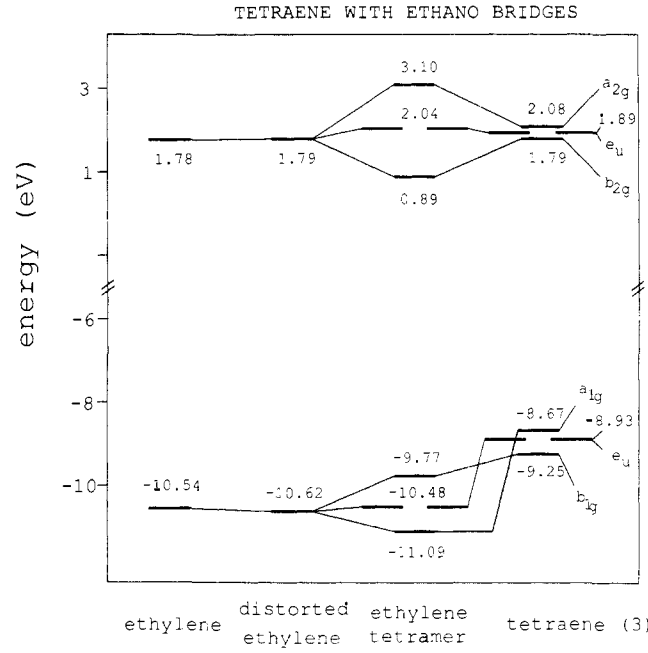

Figure 4. Correlation diagram giving the STO-3G π and π^* orbital energies for the ethylene, ethylene distorted as in **3**, the model ethylene tetramer, and the tetraene **3**.

solutions as the basis set is enlarged. Although this is a serious problem with basis sets containing diffuse functions (e.g., 6-31+G), it is not expected to be a severe problem with the 3-21G basis set. Nonetheless, there is no guarantee that simple MO calculations with the 3-21G basis set give more realistic splittings in the unfilled orbital manifolds than do calculations with the STO-3G basis set. In fact, we suspect, based on comparison between theory and experiment in other systems, that the "truth" lies somewhere in between the STO-3G and 3-21G results. Stabilization calculations[17] which properly handle the coupling to the continuum are required to resolve this problem. Due to the above-mentioned possible problem with the use of the 3-21G basis set for the π^* manifolds, results obtained with the STO-3G basis set are emphasized in this paper, and, unless indicated otherwise, the subsequent discussions pertain to the STO-3G results.

The STO-3G calculations give small ($\lesssim$0.3 eV) splittings for the unfilled π^* orbitals of **1**–**3** and for the filled π orbitals of **1** and **2**. A somewhat larger splitting (0.58 eV) is predicted for the π orbitals of **3**. These results are consistent with the PE data for **1**–**3** and with the ET data for **2** and **3**. Both the experimental and theoretical results would seem to indicate relatively weak interactions among the localized π (or π^*) orbitals in **1**–**3**. However this is not correct: both TB and TS interactions are significant, but they act in opposite directions, with the result that

(17) Hazi, A. U.; Taylor, H. S. *Phys. Rev. A* **1976**, *14*, 2071.

the net splittings are small. This has been shown previously for the π orbitals of **1**.[4] The results of the present investigation show that it is also the case for the π orbitals of **2** and **3** as well as for the π^* orbitals of all three compounds. This can be seen from Table I and Figures 2–4 where the STO-3G results for ethylene, **1**, **2**, and **3**, and the model ethylene "dimer", "trimer", and "tetramer" are summarized. To facilitate comparison with experiment, in constructing the correlation diagrams, the KT EA's of the polyenes have been increased by 6.94 eV, the amount needed to bring the STO-3G KT value of the EA of ethylene into agreement with experiment, and the calculated IP's have been increased by 1.65 eV, the amount by which the STO-3G KT value of the ethylene IP is in error. The calculations on the model dimer, trimer, and tetramer species are carried out both with planar ethylenes and with the ethylene molecules distorted as in **1**, **2**, and **3**. The distortion of the ethylenes proves significant only for the π^* orbital of the dimer. In this case the distortion results in a 0.81 eV decrease in the energy of the π^* orbital.[18]

The STO-3G calculations on the model dimer give a TS splitting of over 3 eV in both the π and π^* orbital spaces. The TS splittings are predicted to be on the order of 2 eV in the model trimer (2.3 and 1.8 eV for the π^* and π orbital spaces, respectively) and smaller still in the model tetramer (2.2 and 1.3 eV in the π^* and π spaces, respectively). The decrease in the TS splittings as one progresses from the ethylene dimer to tetramer (and presumably also along the sequence **1** to **2** to **3**) is due to the decrease in overlap between the $\pi(\pi^*)$ orbitals as the angle between adjacent ethylenic groups is increased. In the model systems, which lack the bridges, the energy ordering of the π and π^* orbitals follows from simple MO considerations: for the ethylene dimer $a_g(\pi)$ is below $b_{1u}(\pi)$ and $b_{3u}(\pi^*)$ is below $b_{2g}(\pi^*)$; for the trimer $a_1'(\pi)$ is below $e'(\pi)$ and $e'(\pi^*)$ is below $a_2'(\pi^*)$; and for the ethylene tetramer $a_{1g}(\pi) < e_u(\pi) < b_{1g}(\pi)$ and $b_{2g}(\pi^*) < e_2(\pi^*) < a_{2g}(\pi^*)$.

The TS splittings obtained from 3-21G calculations on the ethylene dimer, trimer, and tetramer are in fairly good agreement with those obtained with the STO-3G basis set, with the most significant difference being the splitting between the $b_{2g}(\pi^*)$ and $e_u(\pi^*)$ levels of **3**, for which the 3-21G splitting is 0.48 eV larger than the STO-3G value. The TS splittings obtained with 6-31+G basis set (also included in Table I) are nearly identical with those obtained with the 3-21G basis set. The π^* orbitals, and hence the π^* splittings, are not meaningful in the 6-31+G basis set due to these orbitals placing far too much weight on the diffuse "+" functions.

Both our calculations with the STO-3G basis set and those of Honneger et al.[4] with the 4-31G basis set indicate that the two π orbitals of **1** are close in energy. The former give a normal ordering (i.e., a_g below b_{1u}), while the latter give an inverted ordering. Since Honneger et al. used the STO-3G optimized geometry, the different ordering of the π levels in the two calculations must be due to the different basis sets employed. Calculations with much larger basis sets would be required to obtain an unambiguous ordering of such closely spaced orbitals. The order of the orbitals (or states) is not the primary concern of the present study, and the essential point is that TB interactions cause a large destabilization of the $a_g(\pi)$ orbital and a small (0.34 eV) stabilization of the $b_{1u}(\pi)$ orbital, with the result that the two π levels of **1** are close in energy. Comparison of the STO-3G results for **1** and for the model dimer reveals that the TB interactions destabilize the $b_{3u}(\pi^*)$ and stabilize the $b_{2g}(\pi^*)$ orbital of **1**, essentially cancelling out the splitting due to TS interactions and causing the π^* orbitals to be nearly degenerate.

Figures 3 and 4 show that the TB interactions have the same qualitative effect on the π and π^* orbitals of the triene and tetraene as for the diene. The TB interactions destabilize both the $a_1'(\pi)$ and $e'(\pi)$ MO's of the triene, with the destabilization of $a_1'(\pi)$ being much greater, causing it to become the highest occupied molecular orbital (HOMO), in accordance with the assignment of McMurry et al.[5] The resulting level ordering is inverted from the "natural" ordering which would prevail if only TS interactins were important. The $a_2'(\pi^*)$ orbital of the triene is strongly stabilized and the $e'(\pi^*)$ orbital weakly destabilized by TB interactions. However, in this case the TB interactions are not quite strong enough to invert the "natural" order of the π^* orbitals. At the STO-3G level of theory TB interactions also lead to an inverted ordering in the π manifold of the tetraene but a natural ordering in the π^* manifold.

As can be seen from Table I, the 3-21G basis set, like the STO-3G basis set, gives small net splittings in the π manifolds of **1**–**3**. This fact, combined with the observation that the TS splittings between the π levels (estimated from the calculations on the ethylene "clusters") are relatively insensitive to the basis set, leads to the conclusion that the TB contributions to the net π splittings must also be relatively basis set independent. The net splittings in the π^* manifolds are also quite small when the STO-3G basis set is employed but are appreciably larger (0.7 eV for **1** and **2** and 0.6 and 1.0 eV for **3**) with the 3-21G basis set. Most of the changes in the net π^* splittings in going from the STO-3G to the 3-21G basis set are due to differences in the magnitudes of the TB interactions in the two basis sets. We should have been able to resolve in the ET spectra the individual anion states (particularly in the case of **3**) if the splittings were as large as indicated by the calculations. We conclude therefore that the 3-21G basis set overestimates the splittings in the π^* manifold.

IV. Analysis of Results

A. Occupied π Orbitals. In order to gain a better understanding of the origins and magnitudes of the TB interactions, a simple perturbation molecular orbital (PMO) analysis of the interactions is given in this section. In this scheme we consider zeroth-order π_i and π_i^* orbitals localized on the ith ethylenic group and zeroth-order σ and σ^* orbitals, denoted as ϕ_j and ϕ_j^*, localized on the jth "cyclohexane" ring. The ϕ_j and ϕ_j^* orbitals in our treatment are delocalized within a ring and are formed from linear combinations of the localized two-center C–C and C–H σ orbitals of Honneger et al.[4] (Associated with the jth cyclohexane ring there are several ϕ_j and ϕ_j^* orbitals, which will be distinguished later when the need arises.) From the localized ϕ_j and ϕ_j^* basis orbitals we form symmetry-adapted semi-localized molecular orbitals (SLMO's) which include the effects of TS but not TB interactions. The TB interactions are then treated by allowing for mixing between SLMO's. In particular, we consider the π/σ, π^*/σ^*, and π^*/σ mixings. The rationale for restricting the π interactions to the occupied σ orbitals while allowing the π^* orbitals to mix with both the σ and σ^* orbitals has been discussed in recent papers[2] and will be commented on in the Appendix to the present work. The validity of the zero-differential overlap (ZDO) approximation is assumed.

For the diene **1** the symmetry-adapted π and σ orbitals are

$$^{SL}a_g(\pi) = 1/\sqrt{2}(\pi_1 + \pi_2) \quad (1a)$$

$$^{SL}b_{1u}(\pi) = 1/\sqrt{2}(\pi_1 - \pi_2) \quad (1b)$$

$$^{SL}a_g(\sigma) = 1/\sqrt{2}(\phi_3' + \phi_4') \quad (1c)$$

$$^{SL}b_{1u}(\sigma) = 1/\sqrt{2}(\phi_3'' + \phi_4'') \quad (1d)$$

where the two ethylenic groups are numbered 1 and 2 and the two "cyclohexane" rings are numbered 3 and 4. The superscript "SL" is used to distinguish SLMO's from canonical orbitals. Due to symmetry the localized molecular orbitals (LMO's) which lead to a_g and b_{1u} σ-type SLMO's are distinct. In the above scheme the "′" and "″" superscripts are used to designate localized ϕ orbitals which lead to a_g and b_{1u} delocalized SLMO's, respectively. The complete set of occupied SLMO's of a_g and b_{1u} symmetry is given in the paper of Honneger et al.[4] The ϕ' and ϕ'' orbitals and their symmetry-adapted combinations which are most important for understanding the TB interactions in **1** are shown in Figure 5.

(18) In constructing the correlation diagrams we have assumed that inductive effects due to the alkyl groups have negligible effect on the energies of the π and π^* basis levels. Consideration of the inductive effects would cause small changes in the shifts attributed to TB interactions.

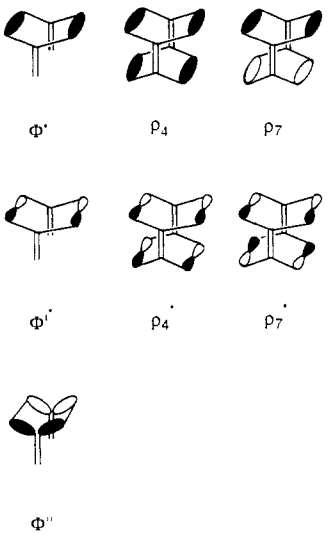

Figure 5. σ LMO's and SLMO's relevant for the discussion of TB interactions.

The second-order perturbation theory (PT) expressions for the shifts in the energies of the π orbitals of the diene due to π/σ mixing are

$$\Delta E(a_g(\pi)) = \sum|\langle {}^{SL}a_g(\pi)|H|{}^{SL}a_g(\sigma)\rangle|^2/\{\epsilon({}^{SL}a_g(\pi)) - \epsilon({}^{SL}a_g(\sigma))\} \quad (2a)$$

$$\Delta E(b_{1u}(\pi)) = \sum|\langle {}^{SL}b_{1u}(\pi)|H|{}^{SL}b_{1u}(\sigma)\rangle|^2/\{\epsilon({}^{SL}b_{1u}(\pi)) - \epsilon({}^{SL}b_{1u}(\sigma))\} \quad (2b)$$

The summations in eq 2a and 2b run over all occupied σ SLMO's of the designated symmetry, and the energies in the denominators are those of the appropriate SLMO's.

From examination of the canonical MO's obtained from the STO-3G calculations it is seen that the $a_g(\pi)$ orbital and the second highest $a_g(\sigma)$ orbital are strongly mixed. The canonical σ orbital in question is dominated by the ρ_4 and ρ_6 SLMO's of Honneger et al. (see Figure 5). The ρ_6 SLMO is primarily C–H bonding in nature and is relatively unimportant with regard to mixing with the $a_g(\pi)$ SLMO. The ρ_4 SLMO, on the other hand, is responsible for nearly 80% of the energy shift in the $a_g(\pi)$ SLMO due to π/σ mixing.[4] The ρ_4 SLMO and the localized orbital (denoted Φ') from which it is derived are sketched in Figure 5. On the basis of the results of our MO calculations and on the findings of Honneger et al., we replace the sum in eq 2a with the single term involving the interaction with the ρ_4 SLMO.

Both our MO calculations and the analysis of Honneger et al. show that $b_{1u}(\pi)/b_{1u}(\sigma)$ mixing is much less important than $a_g(\pi)/a_g(\sigma)$ mixing. The localized Φ' orbital, which dominates the latter interaction, does not lead to a symmetry-adapted b_{1u} orbital. Accordingly, in the analysis of the diene, we neglect π/σ coupling in the b_{1u} symmetry block all together. For the time being we also neglect π/σ^* mixing which, as was noted above, stabilizes the $b_{1u}(\pi)$ SLMO by a small amount. (The role of π/σ^* mixing will be considered in section V and in the Appendix.) To further simplify the PT expressions one additional approximation is made: namely, that the energies of the symmetry-adapted orbitals are replaced with those of the appropriate localized orbitals.[19] (This approximation will also be made in the discussion of the π/σ mixing in **2** and **3** and in the subsequent analysis of the π^*/σ^* and π^*/σ interactions in **1**–**3**).

With the above assumptions we have

$$\Delta E(a_g(\pi)) = |\langle {}^{SL}a_g(\pi)|H|{}^{SL}a_g(\Phi')\rangle|^2/\{\epsilon(\pi) - \epsilon(\Phi')\} \quad (3a)$$

$$\Delta E(b_{1u}(\pi)) = 0 \quad (3b)$$

where ${}^{SL}a_g(\Phi')$ is the a_g SLMO derived from the Φ' LMO. (For the diene this SLMO is just the ρ_4 orbital of Honneger et al.) Defining the interaction between localized π and Φ' orbitals as

$$\gamma = |\langle \pi_i|H|\Phi_j'\rangle|^2/\{\epsilon(\pi) - \epsilon(\Phi')\} \quad (4)$$

and using the wave functions given in eq 1, we obtain

$$\Delta E(a_g(\pi)) = 4\gamma \quad (5)$$

The utility of this result will become apparent when the shifts due to π/σ mixing in the triene and tetraene are derived. From comparison of the STO-3G energies of the $a_g(\pi)$ orbitals of **1** and of the corresponding ethylene dimer we obtain $\gamma = 0.75$ eV. In the remainder of the paper, we refer to the procedure of obtaining estimates of the TB interaction energies from comparing the ab initio results for the molecule of interest to those of the appropriate ethylene *n*-mer as the "TB model".

For the triene **2**, the relevant, symmetry-adapted π and σ orbitals are

$${}^{SL}a_1'(\pi) = 1/\sqrt{3}(\pi_1 + \pi_2 + \pi_3) \quad (6a)$$

$${}^{SL}e'(\pi) = 1/\sqrt{2}(\pi_1 - \pi_2), \quad 1/\sqrt{6}(2\pi_3 - \pi_1 - \pi_2) \quad (6b)$$

$${}^{SL}a_1'(\sigma) = 1/\sqrt{3}(\Phi_4' + \Phi_5' + \Phi_6') \quad (6c)$$

$${}^{SL}e'(\sigma) = 1/\sqrt{2}(\Phi_4' - \Phi_5'), \quad 1/\sqrt{6}(2\Phi_6' - \Phi_4' - \Phi_5') \quad (6d)$$

where π_1, π_2, and π_3 refer to the localized π orbitals and Φ_4', Φ_5', Φ_6' to Φ' orbitals localized on the three cyclohexane rings. The numbering scheme is such that the rings labeled 4, 5, and 6 are opposite the double bonds labeled 1, 2, and 3, respectively.

In eq 6 we have assumed that the π/σ mixing in **2**, like that in **1**, is dominated by SLMO's derived from the Φ' LMO. This assumption is confirmed by examination of the canonical MO's obtained from the STO-3G calculations. Accordingly, the PT expressions giving $\Delta E(a_1'(\pi))$ and $\Delta E(e'(\pi))$ are each restricted to a single term:

$$\Delta E(a_1'(\pi)) = |\langle {}^{SL}a_1'(\pi)|H|{}^{SL}a_1'(\Phi')\rangle|^2/\{\epsilon(\pi) - \epsilon(\Phi')\} \quad (7a)$$

$$\Delta E(e'(\pi)) = |\langle {}^{SL}e'(\pi)|H|{}^{SL}e'(\Phi')\rangle|^2/\{\epsilon(\pi) - \epsilon(\Phi')\} \quad (7b)$$

As for the diene, the interaction between a localized ethylenic π orbital and the Φ' orbital of an adjacent "cyclohexane" moiety is defined as γ. Assuming that only interactions between adjacent ethylenic and cyclohexane entities are important and using the wave functions given in eq 6, it is found that

$$\Delta E(a_1'(\pi)) = 4\gamma \quad (8a)$$

$$\Delta E(e'(\pi)) = \gamma \quad (8b)$$

Thus the TB model predicts that π/σ interactions in the triene destabilize the $a_1'(\pi)$ orbital four times more than they destabilize the $e'(\pi)$ orbital. This compares well with the computed value of 3.6 for $\Delta E(a_1'(\pi))/\Delta E(e'(\pi))$, with the ΔE values being obtained by subtracting the STO-3G orbital energies of the triene from those of the ethylene "trimer".

A similar analysis of the interactions of the π and σ orbitals of the tetraene **3** gives

$$\Delta E(a_{1g}(\pi)) = 4\gamma \quad (9a)$$

$$\Delta E(e_1(\pi)) = 2\gamma \quad (9b)$$

$$\Delta E(b_{1g}(\pi)) = 0 \quad (9c)$$

The PMO model gives $\Delta E(a_{1g}(\pi))/\Delta E(e_u(\pi)) = 2.0$ and $\Delta E(b_{1g}(\pi))/\Delta E(e_u(\pi)) = 0.0$, in fairly good agreement with the corresponding values of 1.6 and 0.3 obtained from the STO-3G calculations.

The calculated shifts in the diene $a_g(\pi)$, triene $a_1'(\pi)$, and tetraene $a_{1g}(\pi)$ levels (relative to the energies of the corresponding

(19) The energy separation between the localized π and Φ' orbitals is about 7 eV, whereas for **1** the energy separation between symmetry-adapted (a_g) and the localized Φ' orbitals is only 5.6 eV. Thus the error associated with the use of the energy of the localized π orbital in eq 3a is about 27%. This approximation introduces smaller errors in the TB shifts of the π levels of **2** and **3**. Similarly, errors of the magnitude of 10–30% are expected due to the use of the energies of the localized rather than symmetry-adapted orbitals in the derivation of eq 10–12.

symmetry-adapted orbitals of the ethylene dimer, trimer, and tetramer) are 3.01, 2.74 and 2.42 eV, respectively. The TB model predicts a shift of 4γ for each of these orbitals. Thus γ decreases as one progresses from the diene to the tetraene, consistent with the decrease in π/Φ' overlap as the angle between the ethylenic and ethano bridging groups increases.

B. Unoccupied π^* Orbitals. In setting up the TB model for the π^* orbitals, both π^*/σ^* and π^*/σ interactions must be considered. This is apparent from the correlation diagrams given in Figures 2–4 from which it is seen that the canonical π^* MO's of **1**, **2**, and **3** (which allow for the mixing with the bridging orbitals) lie in between the lowest and highest lying π^* orbitals of the model ethylene dimer, trimer, and tetramer, respectively. We assume that the π^*/σ interactions are dominated by the SLMO's derived from the same ϕ orbital (Φ') which dominates the π/σ interactions. In the case of **1** the relevant SLMO is the ρ_7 orbital of Honneger et al. It is further assumed that the dominant π^*/σ^* interactions are with the SLMO's derived from the Φ'^* localized orbital shown in Figure 5 and which is the antibonding analogue of the Φ' orbital. In the case of **1** the relevant SLMO is ρ_4^*. Examination of the canonical π^* MO's of **1–3** confirms that Φ' and Φ'^* are the key localized orbitals for understanding TB interactions in the π^* manifolds. The ρ_7 and ρ_7^* SLMO's of **1** are shown in Figure 5.

The second-order interaction energies between a localized ethylenic π^* orbital and the localized Φ' and Φ'^* orbitals of an adjacent ring are denoted by δ and η, respectively. The shifts in the π^* orbital energies due to mixing with the Φ' and Φ'^* orbitals can then be expressed as

diene	triene	tetraene	
$\Delta E(b_{2g}(\pi^*)) = -4\eta$	$\Delta E(a_2'(\pi^*)) = -4\eta$	$\Delta E(a_{2g}(\pi^*)) = -4\eta$	(10a)
$\Delta E(b_{3u}(\pi^*)) = 4\delta$	$\Delta E(e'(\pi^*)) = -\eta + 3\delta$	$\Delta E(e_u(\pi^*)) = -\eta + 2\delta$	(10b)
		$\Delta E(b_{2g}(\pi^*)) = 4\delta$	(10c)

Analysis of the results of the STO-3G calculations gives $\eta = 0.46$, 0.42, and 0.26 eV for **1**, **2**, and **3**, respectively.[20] The corresponding values for δ are 0.35, 0.29, and 0.23 eV. For comparison we note that γ, which gives the shift in the π levels due to π/σ mixing, is 0.75, 0.69, and 0.61 eV for **1**, **2**, and **3**, respectively. These results show that both π^*/σ^* and π^*/σ interactions are sizable and that they are smaller than the π/σ interactions. An analogous situation has been found for compounds **4** and **5**.

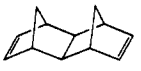

4

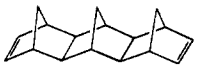

5

The above model, in spite of several simplifying assumptions, accounts quite nicely for the general trends in the energies of the π and π^* levels of **1**, **2**, and **3**. However, it should be noted that its success may be partly due to the fact that the interaction parameters γ, η, and δ (as determined from comparison of the HF calculations on **1**, **2**, and **3** and the model dimer, trimer, and tetramer) actually include the effects of all σ and σ^* orbitals of the relevant symmetry.

V. Determination of γ, η, and δ Parameters from Calculations on Molecular Fragments

In determining the values of the parameters in the TB model, we made use of the results of the ab initio calculations on **1–3**. The utility of the TB model would be enhanced if it were predictive, i.e., did not require performing a MO calculation for each molecule of interest. In this section we show that the parameters in the TB model can be determined from calculations on the 1,4-dimethylenecyclohexane fragment compound **6**. Other than

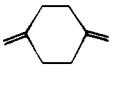

6

(20) For the tetraene η was determined from the shift in the $a_{2g}(\pi^*)$ level and δ from the shift in the $b_{2g}(\pi^*)$ level.

Table II. Comparison of the γ, δ, and η Parameters (eV) Obtained from Calculations on the Fragment Compound **6** and on Compounds **1–3**[a]

parameter	diene	triene	tetraene
γ	0.82 (0.75)	0.73 (0.69)	0.63 (0.61)
δ	0.38 (0.35)	0.31 (0.29)	0.21 (0.23)
η	0.48 (0.46)	0.43 (0.42)	0.23 (0.26)

[a] The first set of numbers in each entry is that obtained from the calculations on the fragment compound, and the results obtained from calculations on **1–3** are given in parentheses.

the CH bond lengths of the terminal CH_2 groups, all geometrical parameters of the fragment are taken to be the same as those of the molecule being modeled, i.e., **1**, **2**, or **3**.

For the three geometries of interest, STO-3G calculations are performed on both the fragment diene **6** and the ethylene dimer, with the two ethylene molecules oriented as in the fragment. The calculations on the dimer are necessary to obtain estimates of the TS splittings. The calculations on **6**, with the geometrical parameters taken from **1**, **2**, or **3**, give values of γ, η, and δ very close to those obtained from MO calculations on the real molecules. This can be seen from examination of the results summarized in Table II.

The values of the γ, η, and δ parameters determined from fragment calculations can be substituted into eq 5, 9, and 10 enabling one to predict the TB shifts in the π and π^* levels of **1–3** due to π/σ, π^*/σ^*, and π^*/σ mixing. These shifts are combined with those due to TS interactions (determined from calculations on the ethylene dimer, trimer, and tetramer) to predict the energies of the π and π^* levels of **1–3**. The energy levels predicted in this manner are compared in Table III with those obtained from the STO-3G calculations on the full molecules. Over all, the agreement is quite good, with the average deviation being less than 0.2 eV.

The largest discrepancy between the results of the full molecule STO-3G calculations and those obtained from the fragment model is for the $b_{1g}(\pi)$ orbital of **3**, for which the fragment model gives an energy of −9.77 eV compared to the −9.25 eV value obtained from the calculations on **3**. The fragment model also leads to too low an energy (by 0.29 eV) of the $e_u(\pi)$ orbital of **3**. We believe that these discrepancies are due to the importance in **3** of the mixing of the π SLMO's with σ SLMO's derived primarily from the localized ϕ orbital designated Φ'' in Figure 5. A sizable discrepancy between the two approaches is also found for the energy of the $b_{1u}(\pi)$ orbital of the diene: use of the parameters from the fragment model give an energy of −8.26 eV as opposed to the −8.60 eV value obtained from the STO-3G calculations on **1**. As mentioned previously, the $b_{1u}(\pi)$ orbital of **1** is stabilized by mixing with the σ^* manifold. This mixing is presumably dominated by the b_{1u} ρ_4^* SLMO derived from the localized Φ'^* orbital shown in Figure 5.

In addition to the above-mentioned interactions, the $b_{1u}(\pi)$ orbital of **1** also mixes with a SLMO derived from the Φ'' LMO, and the $b_{1g}(\pi)$ and $e_u(\pi)$ orbitals of **3** also mix with SLMO's derived from the Φ'^* LMO. The magnitudes of the π/Φ'' and π/Φ'^* interactions vary with geometry in such a way that the former prove most important for **3** and the latter for **1**. The calculations on the fragment compounds can be used to derive a parameter, π, that gives the net effect of the mixing with the SLMO's derived from the Φ'' and Φ'^* LMO's.[21] When both the ω and γ parameters are used in estimating the IP's, the predictions of the $b_{1u}(\pi)$ IP of **1** and the $b_{1g}(\pi)$ and $e_u(\pi)$ IP's of **3** are found to be in excellent agreement with full molecule STO-3G values (see Table III). The localized Φ'' and Φ'^* LMO's which prove

(21) This is accomplished by comparing the STO-3G energies of the $\pi(b_2)$ orbitals of **6** and the ethylene dimer (with the geometry of **6** and the dimer both chosen to correspond to that of the compound of interest, i.e., **1**, **2**, or **3**). The quantity 2ω is associated with this energy difference and includes the mixing of the $\pi(b_2)$ orbital with both σ and σ^* orbitals of the appropriate symmetry. The shift in the $b_{1u}(\pi)$ orbital of **1** and the $b_{1g}(\pi)$ of **3** due to mixing with the appropriate SLMO's derived from the Φ'' and Φ'^* LMO's is then 4ω, while the corresponding shift in the $e_u(\pi)$ orbital of **2** is 2ω.

Table III. Energies (eV) of the π and π^* Orbitals Predicted Using Fragment Molecule Parameters and from Calculations on the Full Molecules **1–3**[a]

	orbital	fragment model[b]	full molecule[c]
diene	$b_{3u}(\pi^*)$	1.18	1.06
	$b_{2g}(\pi^*)$	0.98	1.07
	$b_{1u}(\pi)$	−8.26 (−8.58)	−8.60
	$a_g(\pi)$	−8.65	−8.92
triene	$a_2'(\pi^*)$	1.99	2.05
	$e'(\pi^*)$	1.86	1.82
	$a_1'(\pi)$	−8.70	−8.88
	$e'(\pi)$	−9.10 (−9.08)	−9.06
tetraene	$a_{2g}(\pi^*)$	1.98	2.08
	$e_u(\pi^*)$	1.90	1.93
	$b_{2g}(\pi^*)$	1.73	1.79
	$a_{1g}(\pi)$	−8.57	−8.67
	$e_u(\pi)$	−9.22 (−8.90)	−8.93
	$b_{1g}(\pi)$	−9.77 (−9.13)	−9.25

[a] All orbital energies are corrected as described in the text. [b] The results in parentheses include also the TB interactions described by the ω parameter discussed in section V of the paper. [c] The "full" molecule results are those obtained from HF/STO-3G calculations on **1**, **2**, and **3**.

important in the mixing with the $b_{1u}(\pi)$ orbital of **1** and the $b_{1g}(\pi)$ and $e_u(\pi)$ orbitals of **3** also lead to SLMO's which interact with the $e'(\pi)$ orbital of **2**. However, in this case, the geometry is such that the π/Φ'' and π/Φ'^* interactions approximately compensate for one another, with the result that the ω parameter is very small for **2**.

The results summarized in Table III show that by the use of the results of the parameters determined from calculations on the fragment molecules near quantitative predictions of the energy levels of the full molecules can be made. With the appropriate choices of fragment geometries this scheme can be used, for example, to predict the π IP's and π^* EA's of the pentaene and hexaene analogues of **1–3**.

VI. Replacement of the Ethano Bridges with Trimethylene Bridges

If the relative magnitudes of the TB and TS interactions in **1–3** were altered, then significant net splittings among the π (and π^*) levels could result. Here we consider the effect of replacing the ethano bridges with trimethylene bridges. While the increase in the length of the bridge will clearly reduce the TS interactions, its effect on the TB interactions is less clear a priori.[22] The reason for this is that there are two localized σ and two localized σ^* orbitals of the trimethylene bridges which are important in the π/σ, π^*/σ^*, and π^*/σ interactions.

STO-3G calculations were carried out on the diene **7** and the triene **8** with trimethylene bridges[23] separating the double bonds. The geometries used in these calculations were obtained from MINDO/3 optimizations. Correlation diagrams presenting the energies of the π and π^* orbitals of **7** and **8** are given in Figures 6 and 7. The calculations give significantly larger splittings in the π and π^* manifolds of **7** and **8** than for those of the ethano-bridged analogues (**1** and **2**). For **7** the STO-3G calculations give splittings of 0.73 and 0.79 eV in the π and π^* spaces, respectively; in **8** both the π and π^* manifolds have splittings of about 0.6 eV. The π and π^* orbitals of **7** and **8** are predicted to have natural orderings (i.e., those which would be obtained if TS interactions were to dominate), and, except for the π^* levels of **7**, the net splittings are found to be within 0.3 eV of the TS splittings, estimated from calculations on the corresponding ethylene dimer and trimer models. π/σ mixing is significant in both **7** and **8** but destabilizes all the π levels to roughly the same extent. In the π^* space only the $b_{2g}(\pi^*)$ level of **7** has an energy

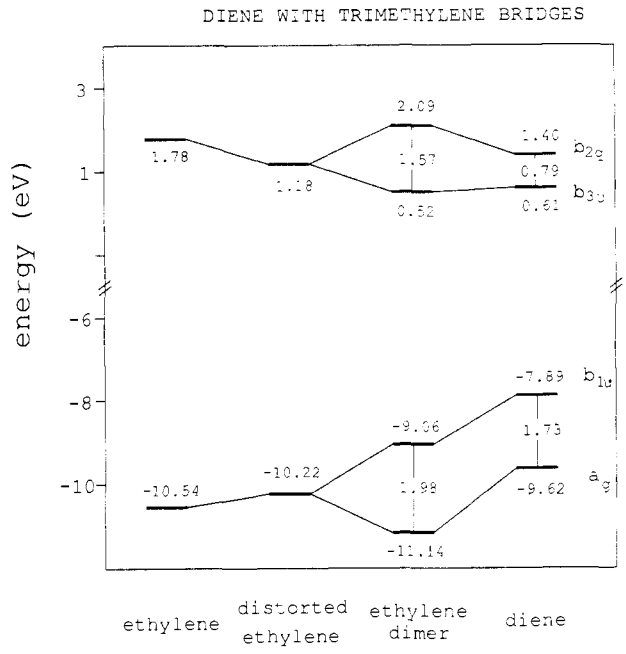

Figure 6. Correlation diagram giving the STO-3G π and π^* orbital energies for ethylene, ethylene distorted as in **7**, the model ethylene dimer (for the geometry of **7**), and the diene **7**.

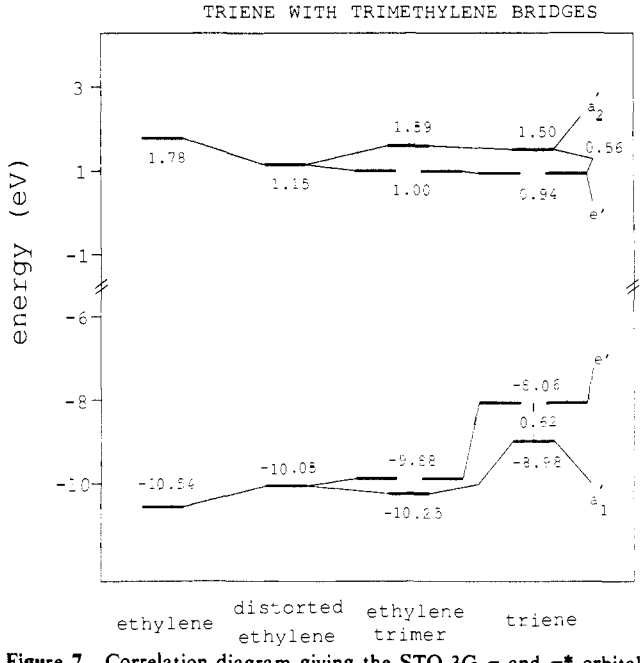

Figure 7. Correlation diagram giving the STO-3G π and π^* orbital energies for ethylene, ethylene distorted as in **8**, the model ethylene trimer (for the geometry of **8**), and the triene **8**.

significantly different from the value predicted in a pure TS model. This does not mean that π^*/σ and π^*/σ^* interactions are unimportant; in fact, both are important, but, except for the $b_{2g}(\pi^*)$ level of **7**, they tend to be of the same magnitude, giving small net shifts. A detailed analysis of the interactions in **7** and **8** will be presented elsewhere.

VII. Conclusions

PE spectroscopic studies have shown that the splittings among the π levels of **1**, **2**, and **3** are small. The ET spectra of **2** and **3** obtained in the present study show that the splittings among the π^* orbitals in these compounds are quite small. Comparison of the results of MO calculations on **1–3** and the model ethylene dimer, trimer, and tetramer species show that both through-space and through-bond interactions are very important in **1–3** but that they oppose one another, causing the net splittings in the π and

(22) Perturbative theoretical expressions for treating TB interactions through trimethylene bridges have been given by Paddon-Row (ref 1), and the papers are cited in ref 2.

(23) The cyclooctane rings in compounds **7** and **8** have boat–boat conformations. It is likely that there are other conformations which are more stable.

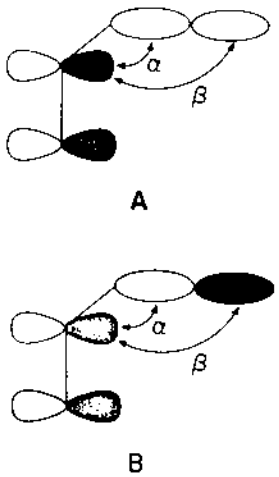

Figure 8. Interactions of a p_π (or p_π^*) orbital with adjacent C–C σ and C–C σ^* orbitals shown in (A) and (B), respectively.

π^* manifolds to be relatively small. As has been found in other classes of compounds, the π orbitals mix strongly with the σ orbitals but relatively weakly with the σ^* orbitals, while the π^* orbitals mix strongly with both σ and σ^* orbitals of the connecting alkane spacer groups.[2] Also, as has been observed in other classes of compounds, the π^*/σ^* interactions in **1**–**3** are slightly greater than the π^*/σ interactions.[24] A model is presented which accounts for the trends in the IP's and EA's for the cyclic polyenes. It is shown that the parameters giving the TB coupling strengths in this model can be determined from calculations on an appropriate fragment compound.

Because the small splittings in the π and π^* manifolds of **1**–**3** are due to the balance between TS and TB interactions, changes which alter the relative importance of these two factors should cause an increase in the splittings. We briefly considered one way of altering this balance, namely, replacing the ethano bridges by trimethylene bridges. By means of STO-3G calculations we showed that compounds with the trimethylene bridges (at least in the conformations considered here) have larger splittings in both the π and π^* manifolds than do their ethano-bridged counterparts.

Acknowledgment. This work was supported with a Grants CHE8207890 (J.E.M.) and CHE8617496 (K.D.J.) from the National Science Foundation and the Australian Research Grants Scheme (M.N.P.R.). The calculations were performed on the Cray X/MP-48 at the Pittsburgh Supercomputing Center.

(24) Paddon-Row, M. N.; Wong, S. S.; Jordan, K. D. *J. Am. Chem. Soc.*, in press.

Appendix: Relative Importance of π/σ and π/σ^* Mixing

In this Appendix we present a simple perturbation theoretical analysis which explains why, in **1**–**3**, both π^*/σ^* and π^*/σ mixing are important while π/σ mixing is much more important than π/σ^* mixing. The Φ' and Φ'^* orbitals which are particularly important in determining TB splittings in the π and π^* manifolds can be viewed as arising from sp^3 hybrid orbitals on the carbon atoms of the ethano bridges. In the C–C σ LMO the two hybrids are in phase (Figure 8A), while in the C–C σ^* LMO they are out of phase (Figure 8B). This causes the $\langle\pi|H|\sigma^*\rangle$ and $\langle\pi^*|H|\sigma^*\rangle$ matrix elements to be smaller than the corresponding $\langle\pi|H|\sigma\rangle$ and $\langle\pi^*|H|\sigma\rangle$ matrix elements. If we make the approximations that

$$\langle\pi_i|H|\sigma_i\rangle = A = \langle\pi_i^*|H|\sigma_j\rangle \quad \text{(A1a)}$$

$$\langle\pi_i|H|\sigma^*\rangle = B = \langle\pi_j^*|H|\sigma_j^*\rangle \quad \text{(A1b)}$$

and

$$|\epsilon_\pi - \epsilon_\sigma| = \Delta_1 = |\epsilon_{\pi^*} - \epsilon_{\sigma^*}| \quad \text{(A2a)}$$

$$|\epsilon_{\pi^*} - \epsilon_\sigma| = \Delta_2 = |\epsilon_\pi - \epsilon_{\sigma^*}| \quad \text{(A2b)}$$

the four relevant interactions become

$$\Delta E(\pi/\sigma) = A^2/\Delta_1 = \gamma \quad \text{(A3a)}$$

$$\Delta E(\pi/\sigma^*) = B^2/\Delta_2 \quad \text{(A3b)}$$

$$\Delta E(\pi^*/\sigma) = A^2/\Delta_2 = \delta \quad \text{(A3c)}$$

$$\Delta E(\pi^*/\sigma^*) = B^2/\Delta_1 = \eta \quad \text{(A3d)}$$

B^2/Δ_2, which provides a measure of the π/σ^* interaction, can then be rewritten as

$$\Delta E(\pi/\sigma^*) = B^2/\Delta_2 = (B^2/\Delta_1)(A^2/\Delta_1)^{-1}(A^2/\Delta_2) = \delta\eta/\gamma \quad \text{(A4)}$$

With use of the values of δ, η, and γ determined in section IV, this expression gives $\Delta E(\pi/\sigma^*)$ values of 0.21, 0.16, and 0.10 eV for **1**, **2** and **3**, respectively. As expected, these estimates of $\Delta E(\pi/\sigma^*)$ are considerably smaller than the $\Delta E(\pi/\sigma)$ values. The stabilization of the $b_{1u}(\pi)$ orbital of **1** predicted by eq A4 is significantly larger than that determined from the STO-3G calculations on **1** and the ethylene dimer. Hence, while the above analysis shows that the π/σ^* interactions are less important than the π/σ interactions, it is too simplistic as it leads to too large a contribution for the π/σ^* mixing.

Registry No. **1**, 77422-56-1; **1** radical anion, 124125-71-9; **2**, 91266-48-7; **2** radical anion, 124125-72-0; **3**, 99922-00-6; **3** radical anion, 124125-73-1; **7**, 124125-74-2; **7** radical anion, 124125-75-3; **8**, 104374-27-8; **8** radical anion, 124125-76-4.